

SUPPLEMENTARY MATERIAL

Exploring the formation kinetics of octacalcium phosphate from alpha-tricalcium phosphate: synthesis scale-up, determination of transient phases, their morphology and biocompatibility

Ilijana Kovrlija¹, Ksenia Menshikh², Olivier Marsan³, Christian Rey³, Christèle Combes³, Janis Locs^{1,4}, Dagnija Loca^{1,4*}

¹Rudolfs Cimdins Riga Biomaterials Innovation and Development Centre, Institute of General Chemical Engineering, Faculty of Materials Science and Applied Chemistry, Riga Technical University, Pulka 3, LV-1007 Riga, Latvia

²Center for Translational Research on Autoimmune and Allergic Disease—CAAD, Department of Health Sciences, Università del Piemonte Orientale, 28100 Novara, Italy

³CIRIMAT, Université de Toulouse, CNRS, Toulouse INP - ENSIACET, 4 allée Emile Monso, CEDEX 4, 31030 Toulouse cedex 4, France

⁴Baltic Biomaterials Centre of Excellence, Headquarters at Riga Technical University, LV-1007 Riga, Latvia

*corresponding author: Fax: +37167089619, Tel.: +371 67089628, e-mail: dagnija.loca@rtu.lv

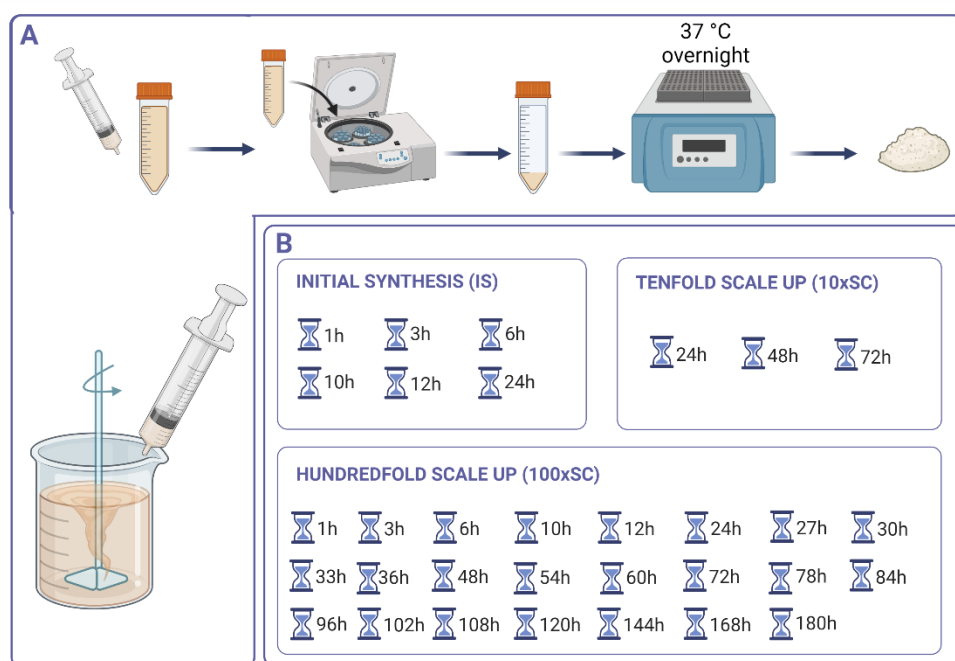


Figure S1. OCP formation from α -TCP suspension – follow-up methodology: A) Acquisition of the samples needed for determining the OCP formation B) Observed time points in the formation of OCP from α -TCP depending on the scale-up level (Created in BioRender.com).

Table S1. List of all the analyzed samples collected at different time points and their presentation within the main manuscript and the supplementary information (S).

Main manuscript			Supplementary information (S)		
Initial synthesis (IS)	Tenfold scale-up (10xSC)	Hundredfold scale-up (100xSC)	Initial synthesis (IS)	Tenfold scale-up (10xSC)	Hundredfold scale-up (100xSC)
24 h final OCP	72 h final OCP	1 h	1 h	24 h	3 h
		24 h			6 h
		30 h			10 h
		3 h	12 h		
			27 h		
			33 h		
		48 h	6 h	48 h	36 h
		78 h			54 h
		96 h			60 h
					72 h
144 h	10 h	72 h final OCP		84 h	
180 h final OCP			102 h		
			108 h		
	120 h				
168 h					

1. α -TCP powder phase and composition characterization

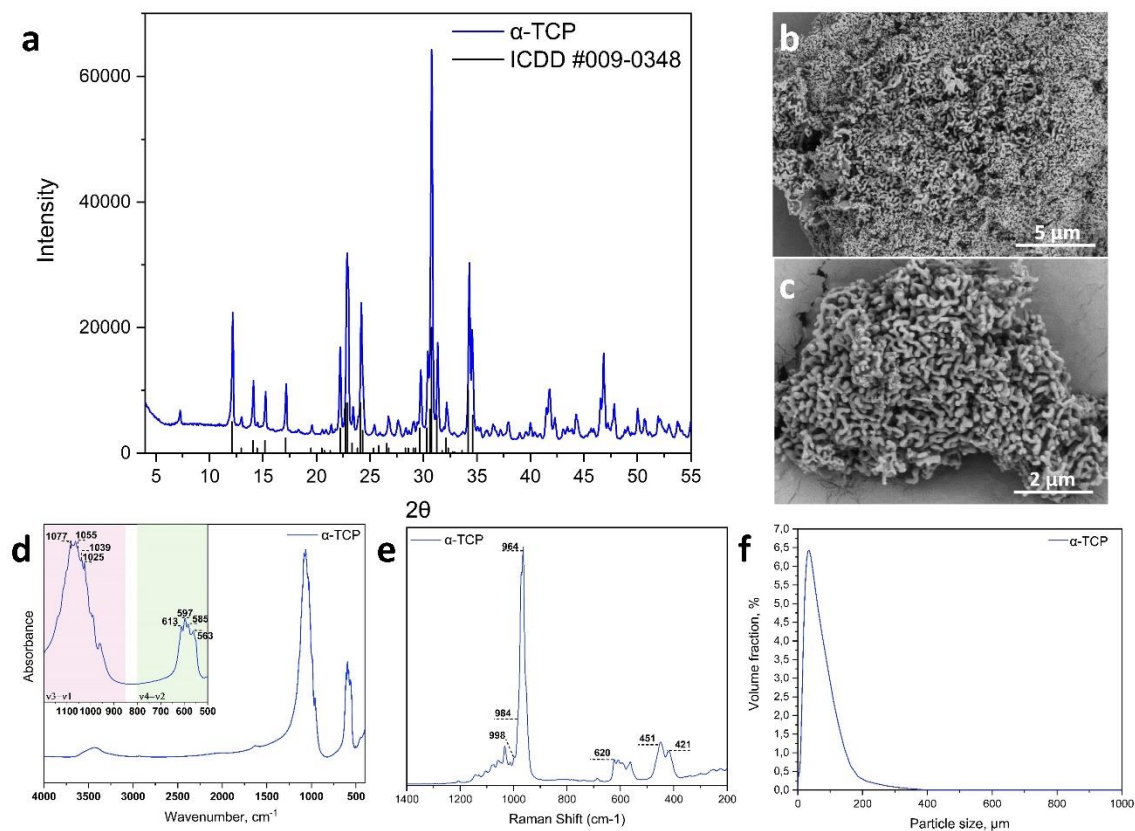


Figure S2. Characterization of the starting α -TCP powder by (a) XRD, (b and c) SEM, (d) FTIR and (e) Raman spectroscopy, and (f) laser granulometry. The corresponding #009-0348 in (a) simulated α -TCP

pattern from the ICDD entry. Pink shading in d) corresponds to $\nu_{1,3}$ PO₄ region and green shading in d) corresponds to $\nu_{2,4}$ PO₄ region.

2. X-RAY DIFFRACTION ANALYSIS

2.1 XRD Initial synthesis (IS)

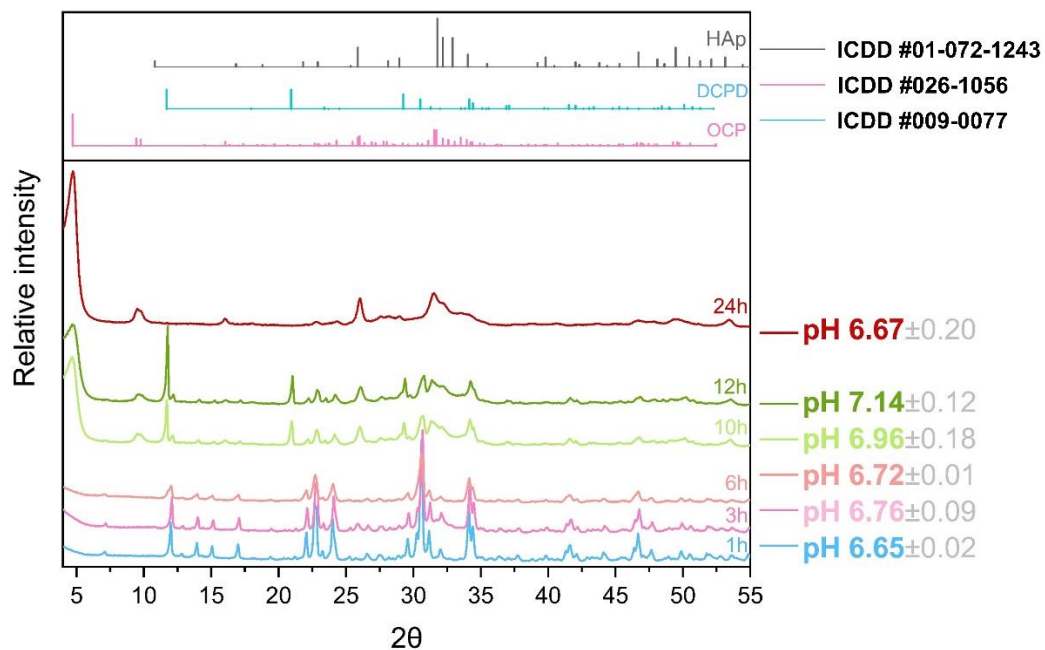


Figure S3. XRD pattern of the specimens collected at different time points during 24 h of IS, with principal phase reference XRD patterns attained from ICDD (#009-0348 for α -TCP; #026-1056 for OCP, #01-072-1243 for HAp, #009-0077 for DCPD).

2.2 XRD Tenfold scale-up (10xSC)

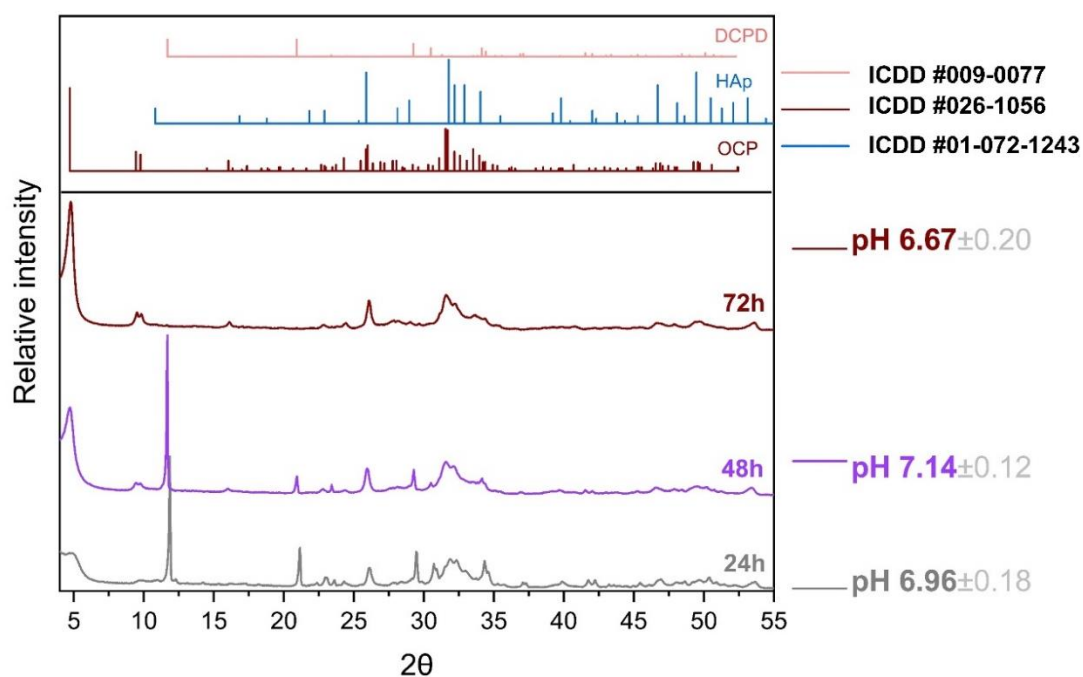


Figure S4. XRD pattern of the specimens collected at different time points during 72 h of 10xSC, with principal phase reference XRD patterns attained from ICDD (#009-0348 for α -TCP; #026-1056 for OCP, #01-072-1243 for HAp, #009-0077 for DCPD).

2.3 XRD Hundredfold scale-up (100xSC)

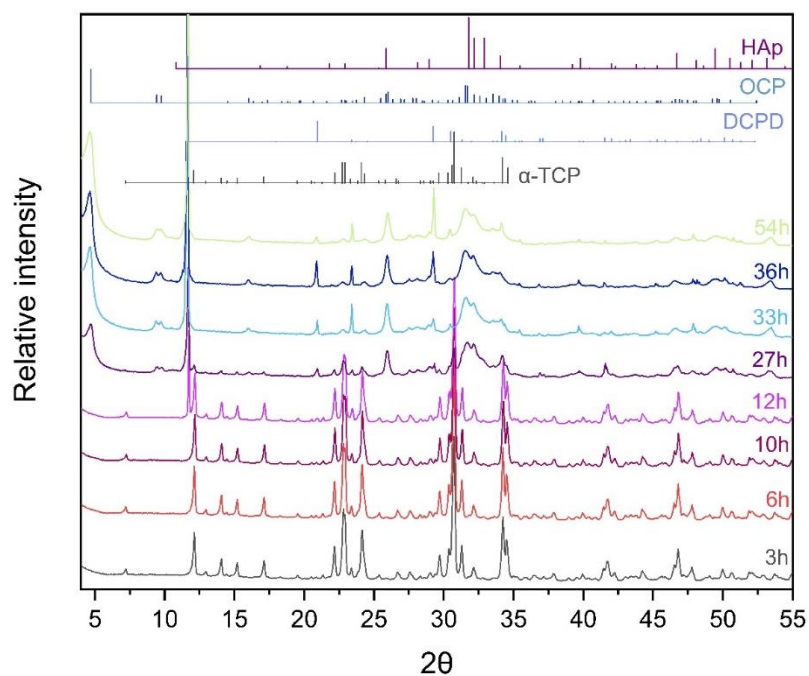


Figure S5. XRD pattern of the specimens collected at different time points from 3 to 54 h during 100xSC and principal phase reference XRD patterns attained from ICDD (#009-0348 for α -TCP; #026-1056 for OCP, #01-072-1243 for HAp, #009-0077 for DCPD).

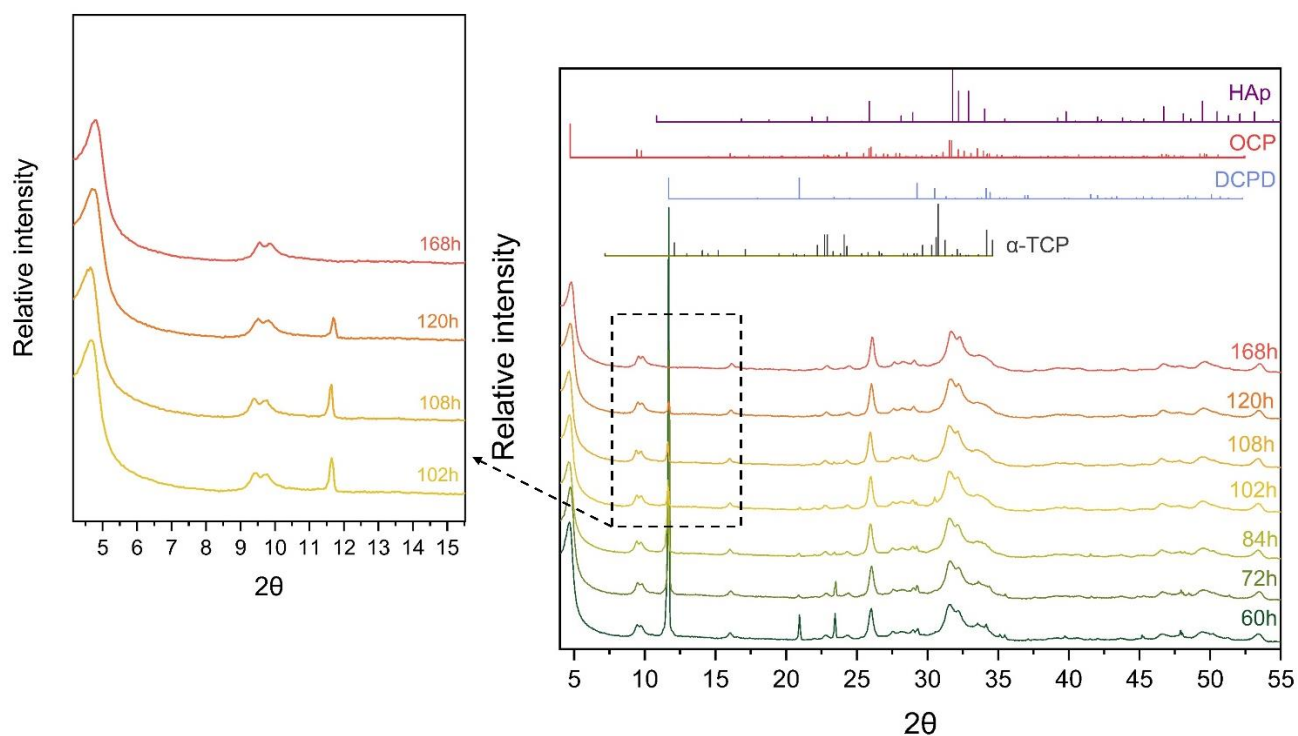


Figure S6. XRD pattern of the specimens collected from 60 to 168 h during 100xSC, and principal phase reference XRD patterns attained from ICDD (#009-0348 for α -TCP; #026-1056 for OCP, #01-072-1243 for HAp, #009-0077 for DCPD).

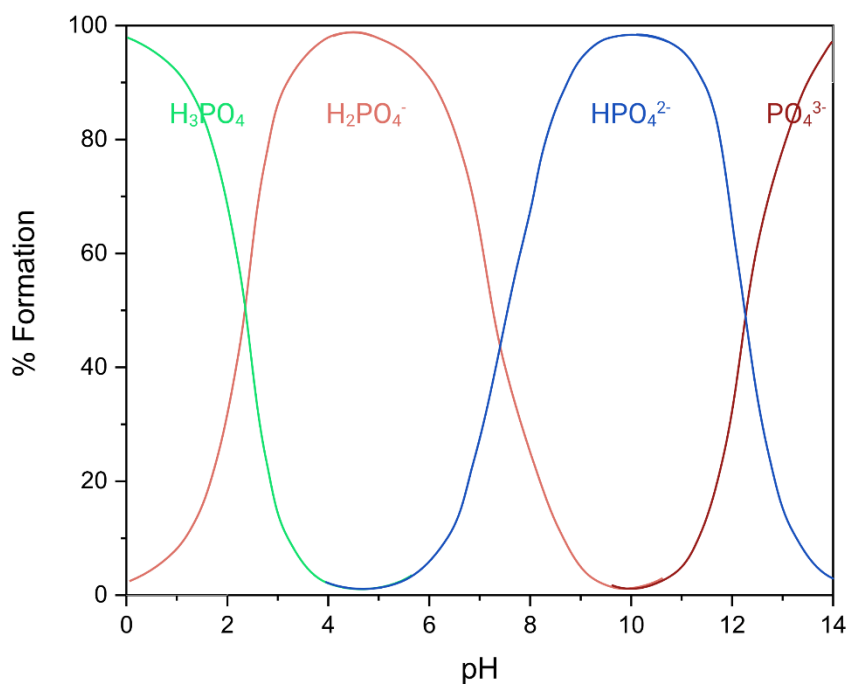


Figure S7. Speciation of orthophosphate species according to the pH. Drawing adopted from Wikipedia.

3. FTIR SPECTROSCOPY ANALYSIS

Table S2. FTIR and Raman band assignments for OCP, α -TCP and DCPD (s-strong, m-medium, sh-shoulder, b-broad, w-weak, v-very, *also $\nu_3\text{PO}_4$ stretch) [34,41–45].

Band assignment	α -TCP		DCPD		OCP	
	FTIR	Raman	FTIR	Raman	FTIR	Raman
$\nu_2 \text{HPO}_4(5)$ bending						356 w 413 m, sh
$\nu_2 \text{PO}_4$ bend	415 w 454 w	421 w 451 w	400 m 418 sh	381 w 411 w	449 vw 466 vw	426 m 450 m
$\nu_4 \text{HPO}_4$ bend					524 w	527 w 556 vw 578 m
$\nu_4 \text{PO}_4$ bend	551 m 563 m 585 m 597 m	577 593 610 w 620 w	526 s 577 m	525 w 588 w	560 m 578 m 601 m	578 m 591 m 609 mw 618 sh
$\text{HPO}_4(5)$ [P-(OH) stretch]					872 w	879 w
$\text{HPO}_4(6)$ [P-(OH) stretch]			872 m	878 m	917 w	916 w
$\nu_1 \text{PO}_4$ stretch	954 m	964 s 976 s	987 s	986 s	962 w 967 w	957 vs 966 s
$\nu_1 \text{HPO}_4$ stretch					1000vw	1005 w 1010sh
$\nu_3 \text{PO}_4$ stretch	984 s 997 s 1013 s 1025 s 1039 s 1055 s	1015 w 1027 vw 1058 vw 1077 vw	1000sh 1060 s 1070 s	1061 m 1079 w	1023 s 1037 s 1055 s 1077 s 1093 s	1011 m 1026vw 1036vw 1048 w 1079vw
$\nu_3 \text{HPO}_4$					1077 s* 1093 s*	1079vw
$\nu_3 \text{HPO}_4(5)$ stretch					1108 s	1109vw
$\nu_3 \text{PO}_4$ stretch				1119vw		
$\nu_3 \text{HPO}_4(6)$ stretch					1121 s*	
$\nu_3 \text{PO}_4$ stretch			1132 s			
$\nu_3 \text{HPO}_4$ stretch					1138vw	
$\text{HPO}_4(5)$ (OH in-plane bend)					1193 w	
$\nu_3 \text{PO}_4$ stretch			1215 m			
$\text{HPO}_4(6)$ (OH in-plane bend)					1295vw	
$\text{HPO}_4(6)$ (OH stretch)					2400 vw,b	
$\nu_{\text{sy}}, \nu_{\text{as}}$ stretch of H-bonded H_2O			3145 s 3278 s 3451 s 3500vb		3500vb	

3.1 Initial synthesis (IS)

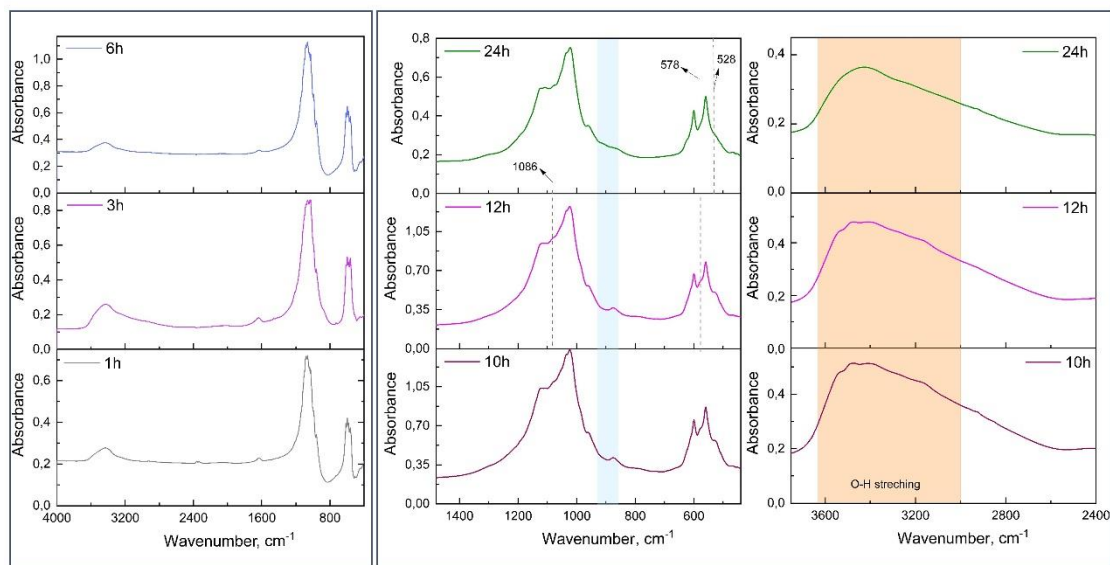


Figure S8. FTIR absorbance spectrum of specimens collected at different time points during the 24 h of IS. Light blue shadowed area is marking the narrow range of HPO_4 (5, 6) P-OH stretch and light orange shadowed area of O-H stretching.

3.2 Tenfold scale up (10xSC)

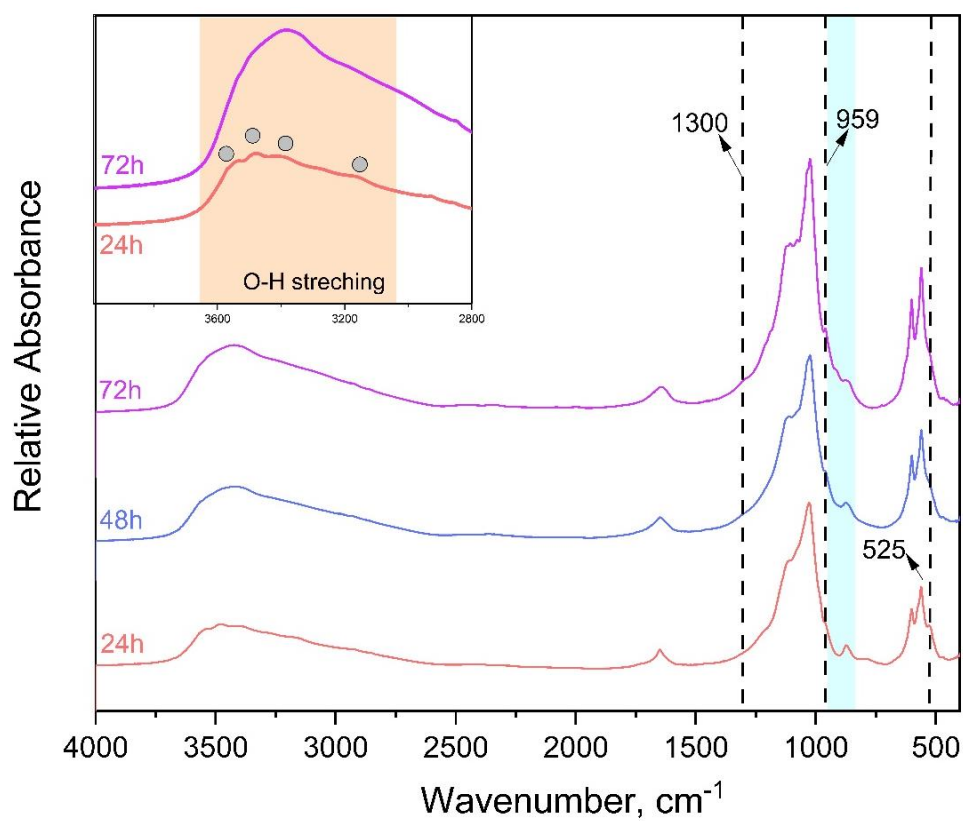


Figure S9. FTIR absorbance spectrum of powders collected at 24, 48 and 72 h of 10xSC. Blue shadowed area is marking the narrow range of HPO_4 (5, 6) P-OH stretch and light orange shadowed area corresponds to O-H stretching (gray circle DCPD).

3.3 Hundredfold scale up (100xSC)

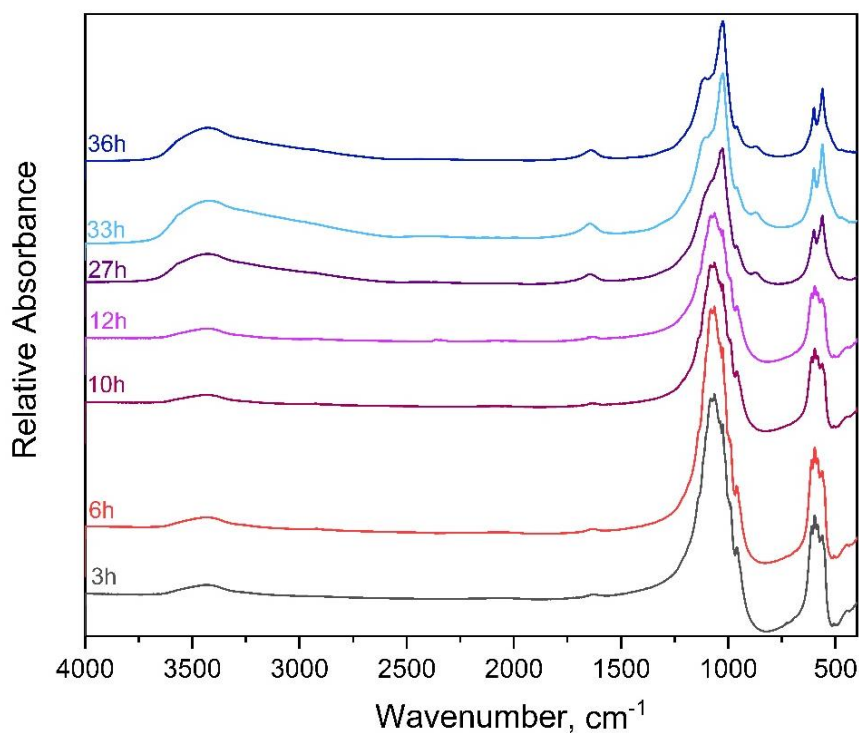


Figure S10. FTIR absorbance spectrum of powders collected at different time points during 36 h of 100xSC. The missing time points (1 h, 24 h) have been disclosed in the main manuscript.

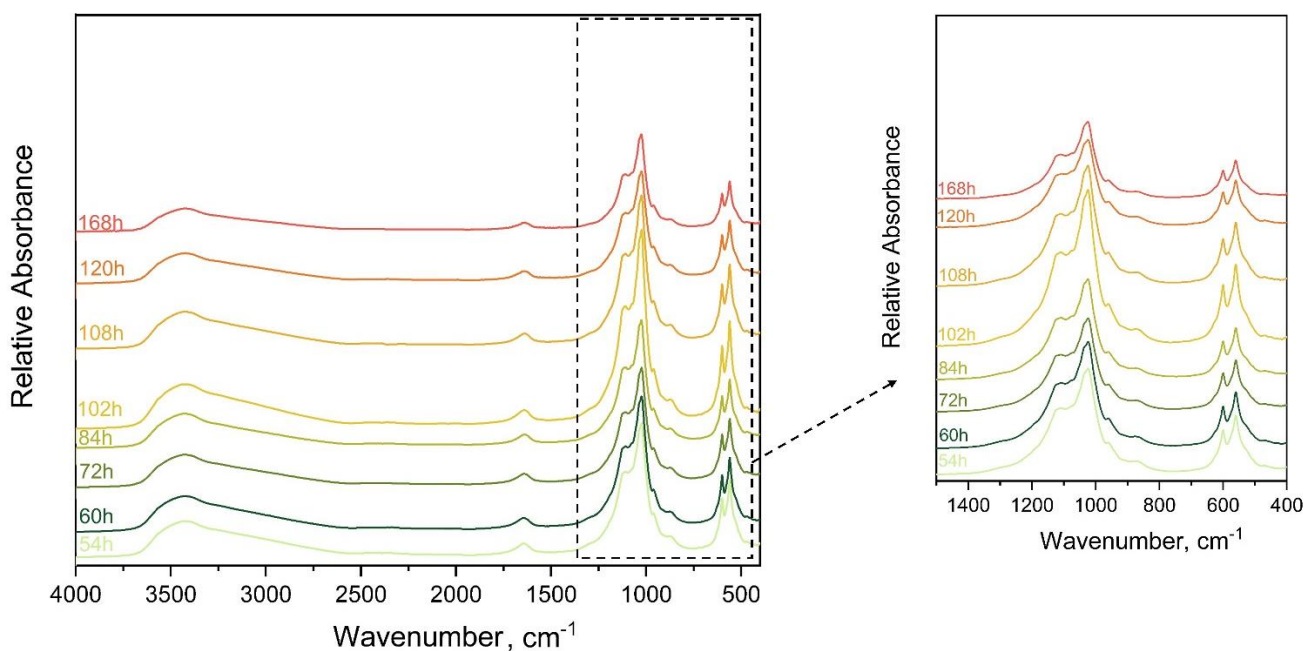


Figure S11. FTIR absorbance spectrum of specimens collected at different time points during the period from 54 h – 168 h of 100xSC. The missing time points (78 h, 96 h, 144 h and 180 h) have been disclosed in the main manuscript.

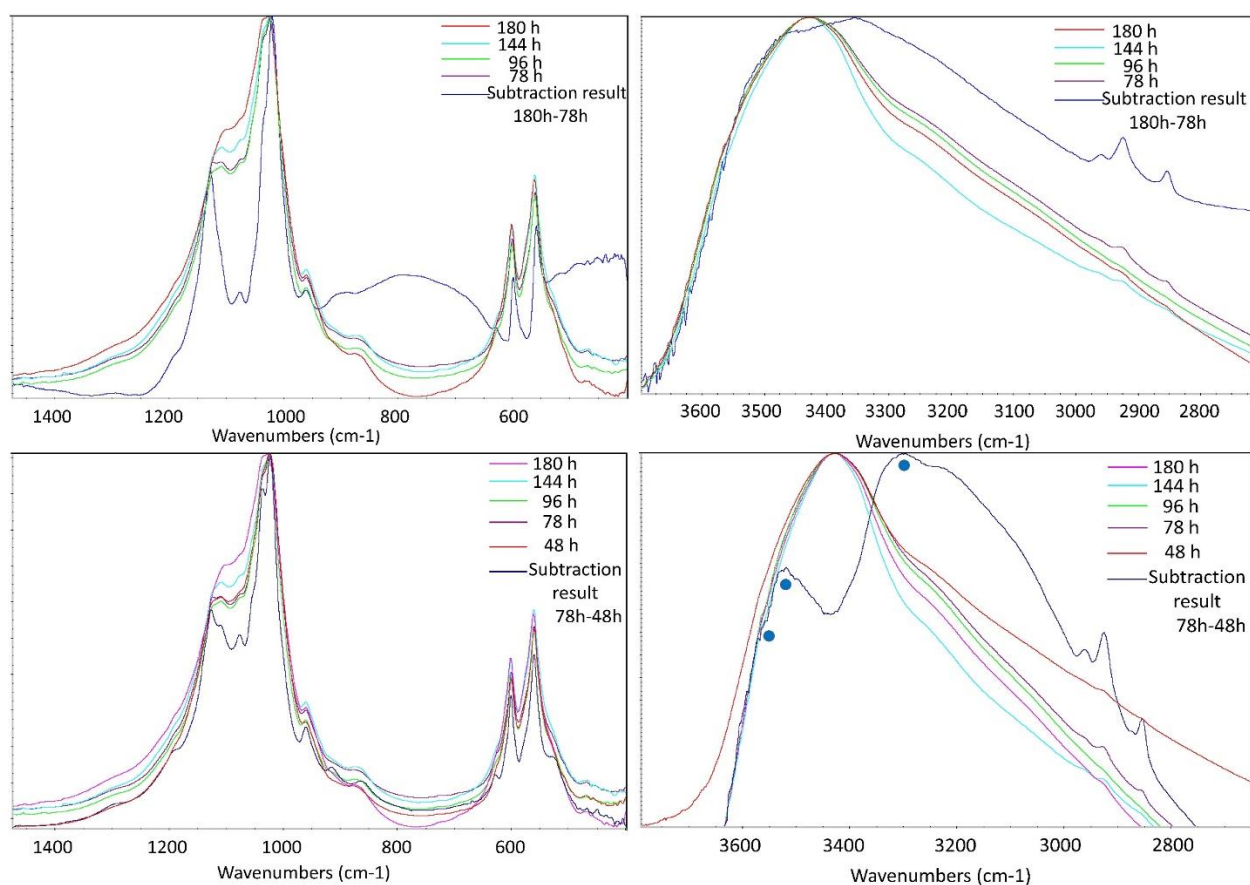


Figure S12. FTIR subtraction absorbance band between 100xSC 78 h and 180 h samples (upper row) and FTIR subtraction absorbance band between 100xSC 48 h and 78 h samples. Blue circles are marking the possible position of DCPD absorption bands.

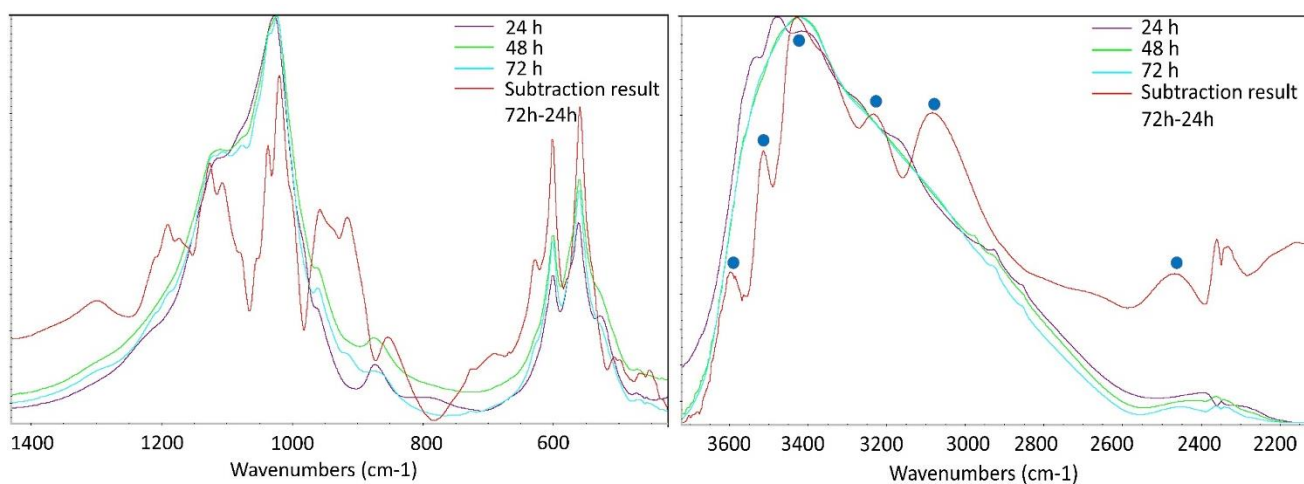


Figure S13. FTIR subtraction absorbance band between 10xSC 24 h and 72 h samples. Blue circles are marking the possible position of DCPD absorption bands.

4. RAMAN SPECTROSCOPY ANALYSIS

4.1 Initial synthesis (IS)

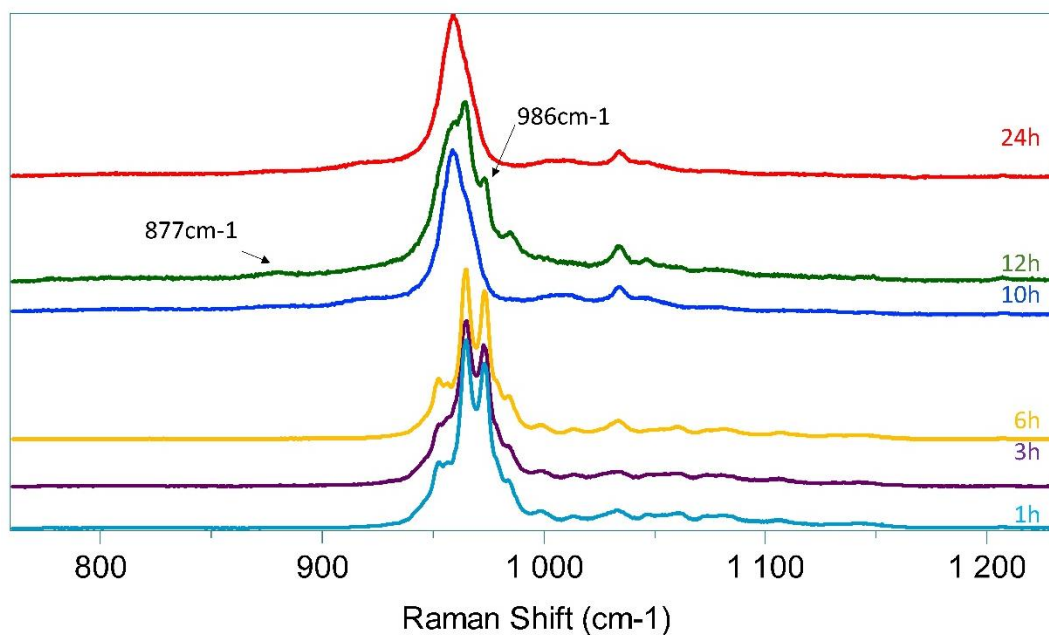


Figure S14. Raman spectra of the powders collected at different time points during initial synthesis (IS). The graph displays a close up of ν_1 stretching mode of the P – O vibration with marked band positions at 877 cm⁻¹ and 986 cm⁻¹.

4.2 Tenfold scale-up (10xSC)

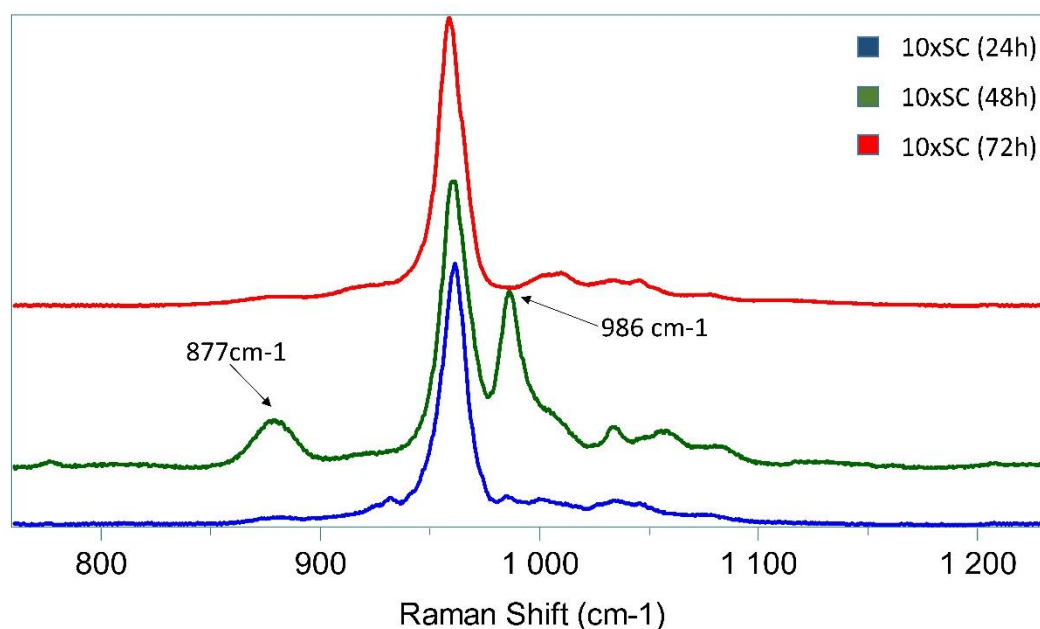


Figure S15. Raman spectra of the powder evolution as a function of time in 10xSC synthesis. The graph displays a close up of ν_1 stretching mode of the P – O vibration with marked band positions at 877 cm⁻¹ and 986 cm⁻¹.

4.3 Hundredfold scale-up (100xSC)

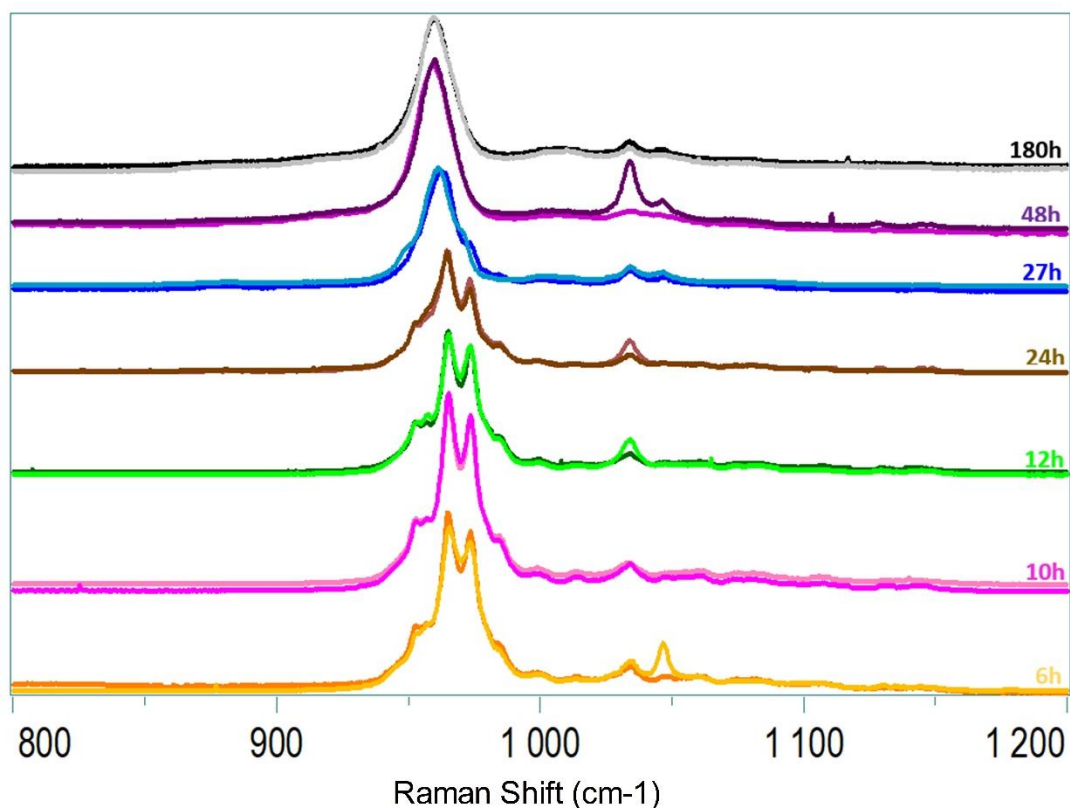


Figure S16. Raman spectra comparison between micro (light color) and macro spot (dark color) of the powders collected during 100xSC.

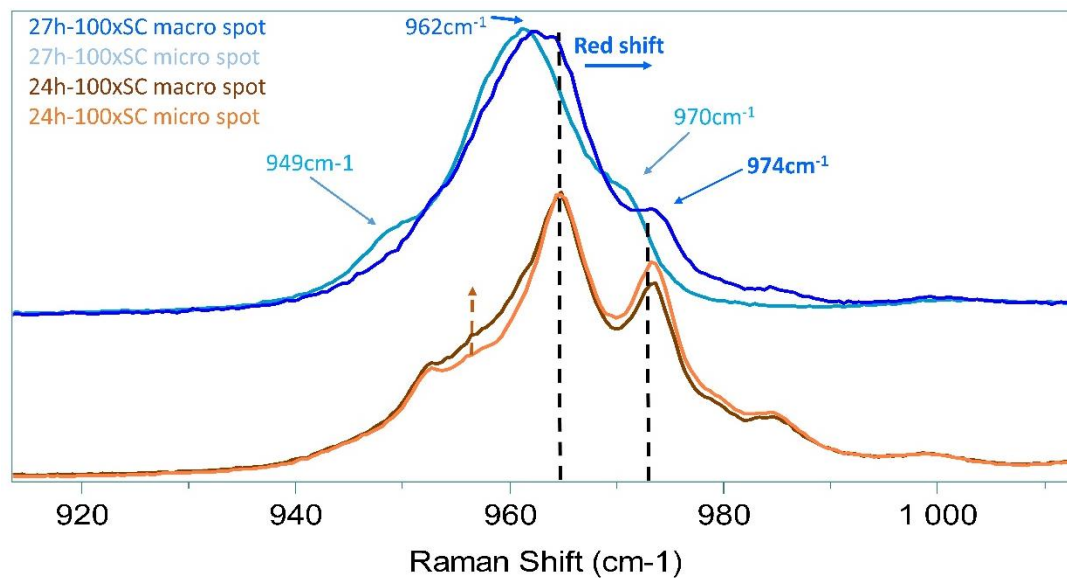


Figure S17. Raman spectra comparison between micro (light color) and macro spot (dark color) of the powders collected after 24 h and 27 h during 100xSC.

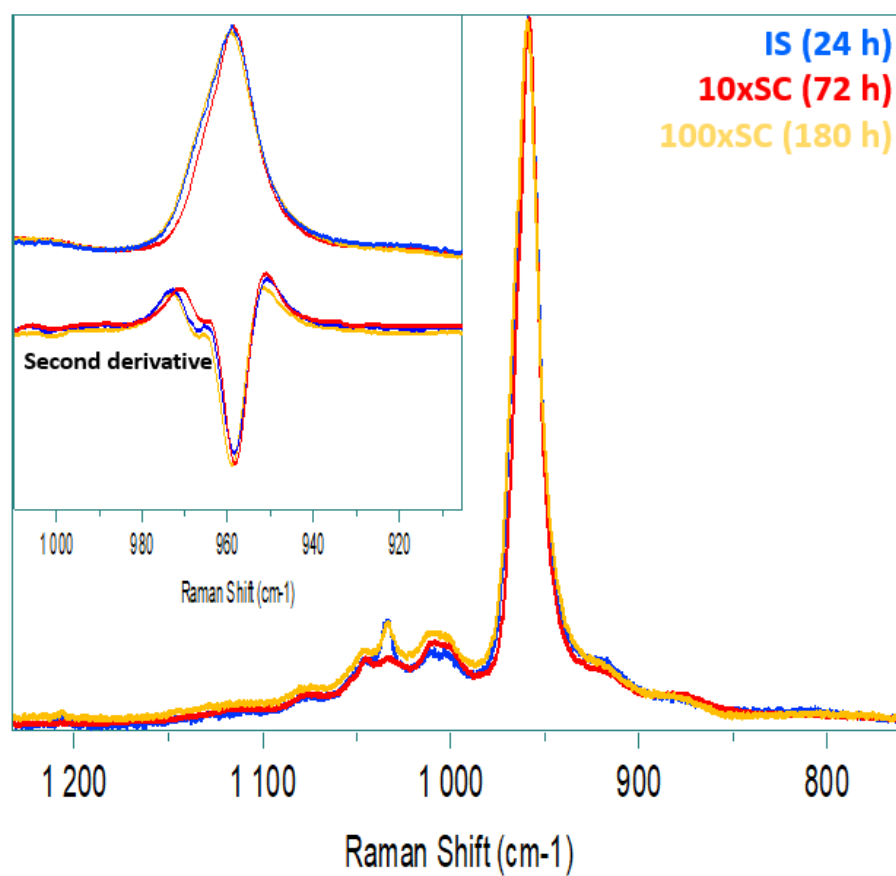


Figure S18. Raman spectra of final OCP phases obtained in three levels of scale-up and the representation of the second derivative of the most prominent band at 958 cm^{-1} .

5. SCANNING ELECTRON MICROSCOPY ANALYSIS

5.1 Initial synthesis (IS)

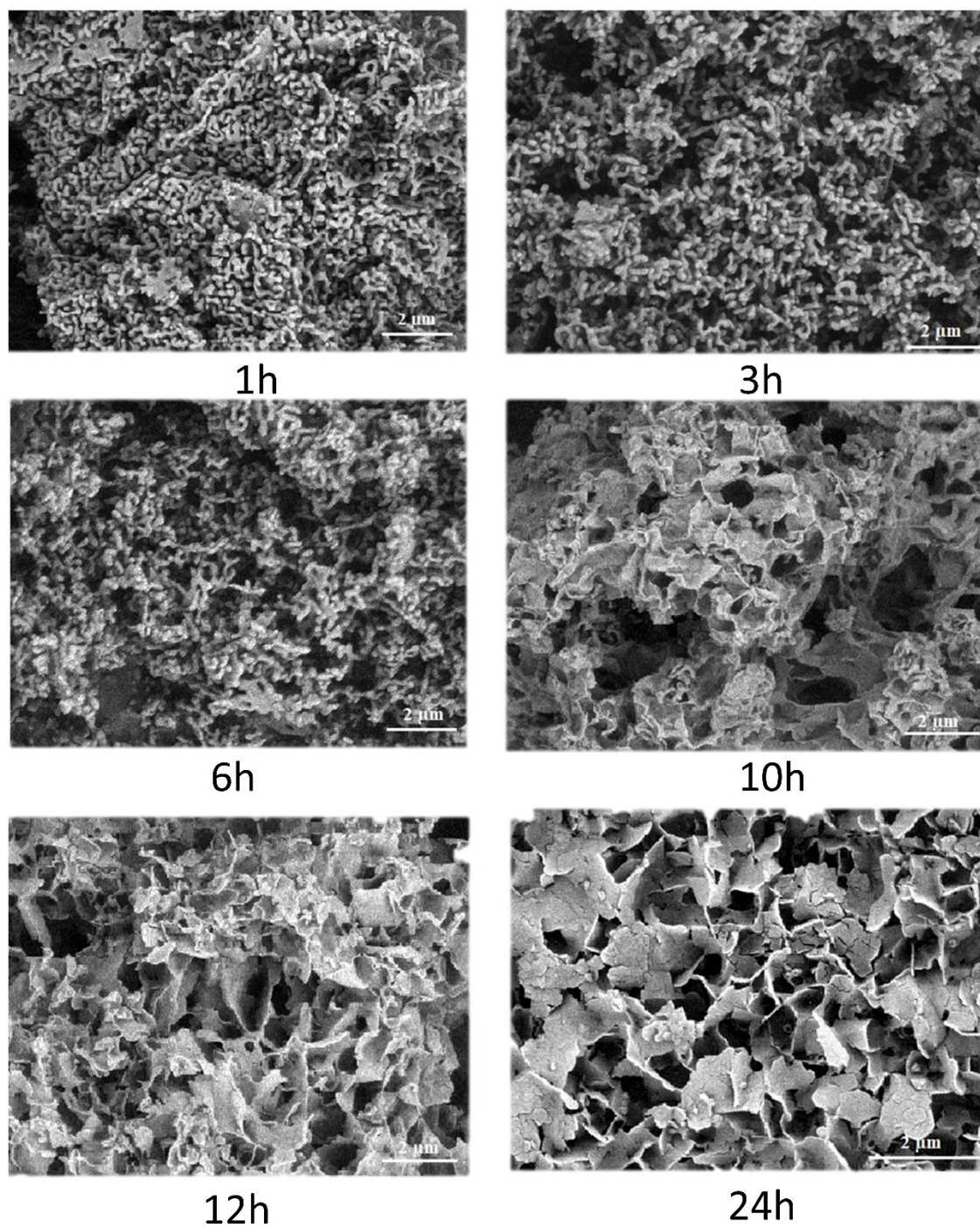


Figure S19. Scanning electron micrographs of α -TCP transformation to OCP (initial synthesis), observed at specific time points indicated below each SEM image. Scale bar 2 μ m.

5.2 Tenfold scale-up (10xSC)

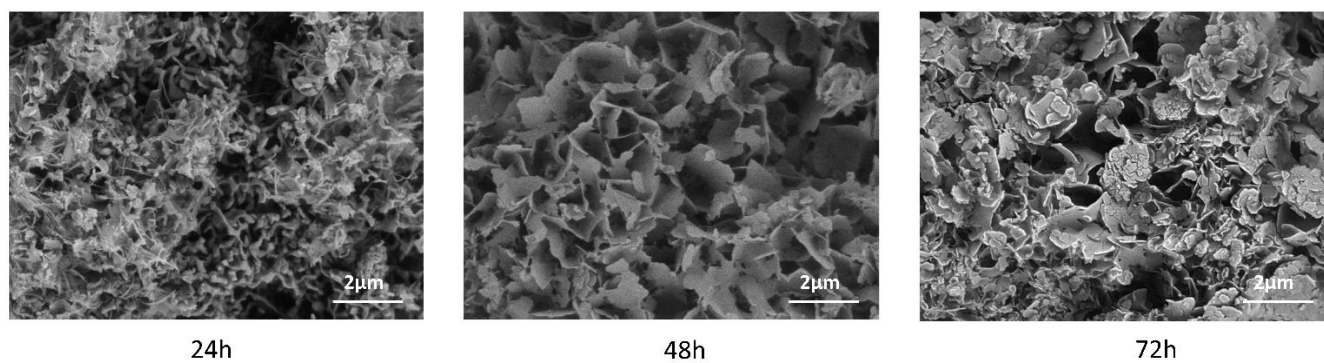


Figure S20. Scanning electron micrographs of α -TCP transformation to OCP (10xSC), observed at specific time points indicated below each SEM image. Scale bar 2 μ m.

6. LASER GRANULOMETRY

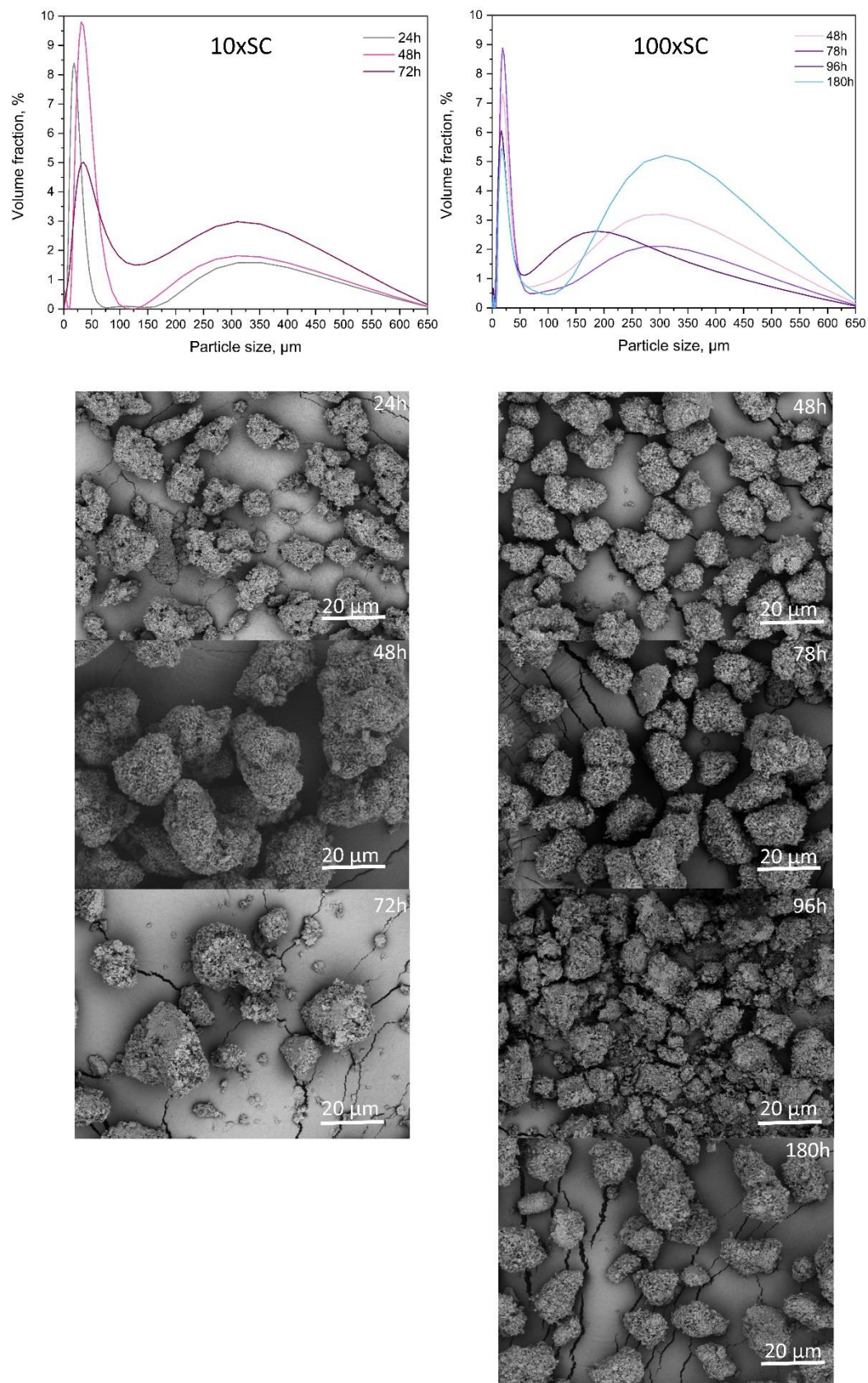


Figure S21. Particle size distribution and SEM micrographs of powders collected at different time points during 10xSC and 100xSC, showing the presence of agglomerated crystals (scale bar 20 μm).

7. CELL PHENOTYPE MORPHOLOGY

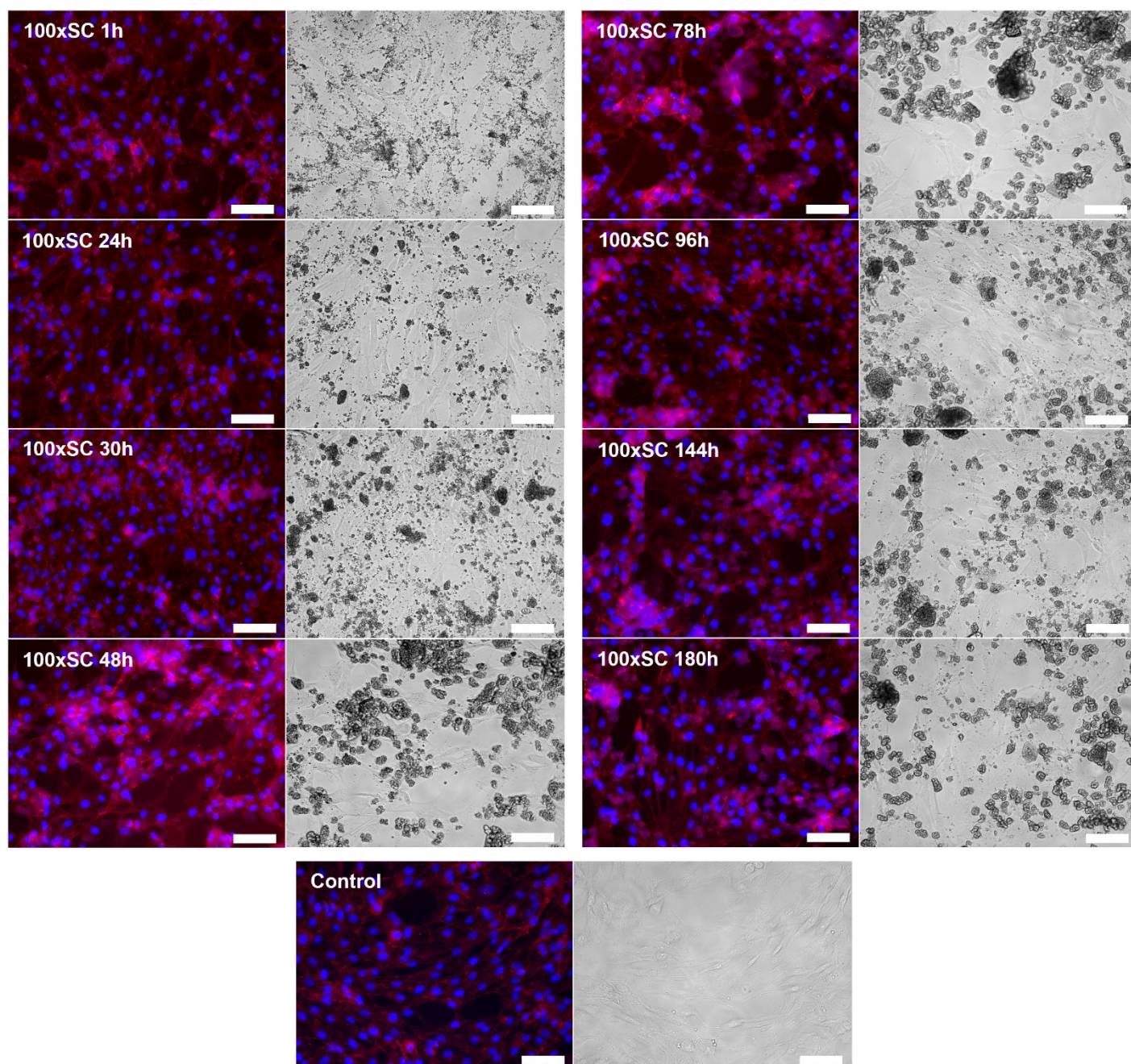


Figure S22. hBMSCs morphology on the third day of cultivation in direct contact with hundredfold synthesis OCP samples in the concentration of 0.5 mg/mL. *Control* represents cells on polystyrene. Immunofluorescent (DAPI – blue, phalloidin – red) and bright-field microscopy. Image bar scale: 125 μ m.

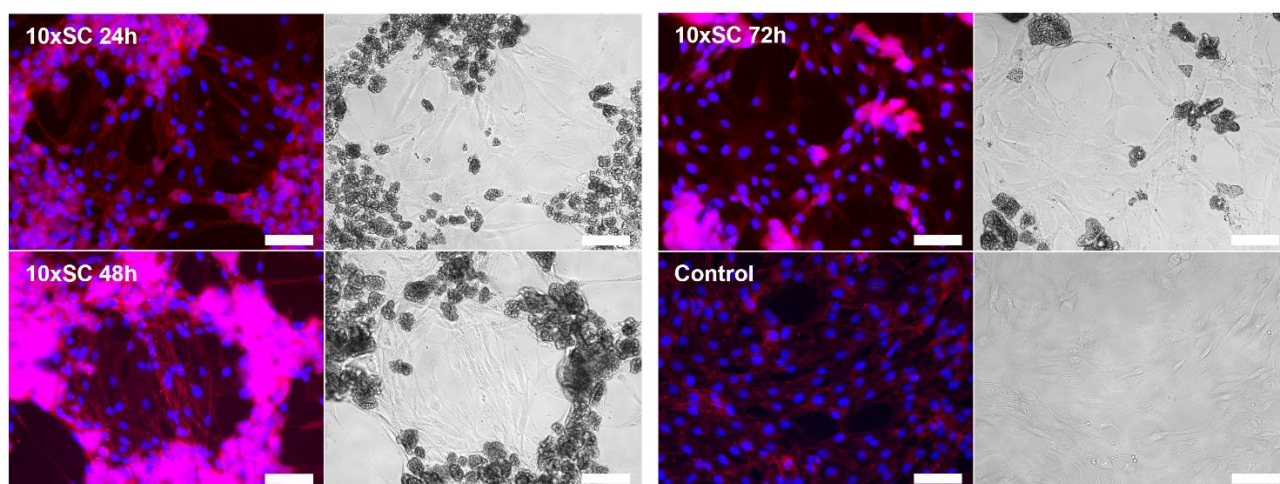


Figure S23. hBMSCs morphology on the third day of cultivation in direct contact with ten-fold synthesis OCP samples in the concentration of 0.5 mg/mL. *Control* represents cells on polystyrene. Immunofluorescent (DAPI – blue, phalloidin – red) and bright-field microscopy. Image bar scale: 125 μ m.

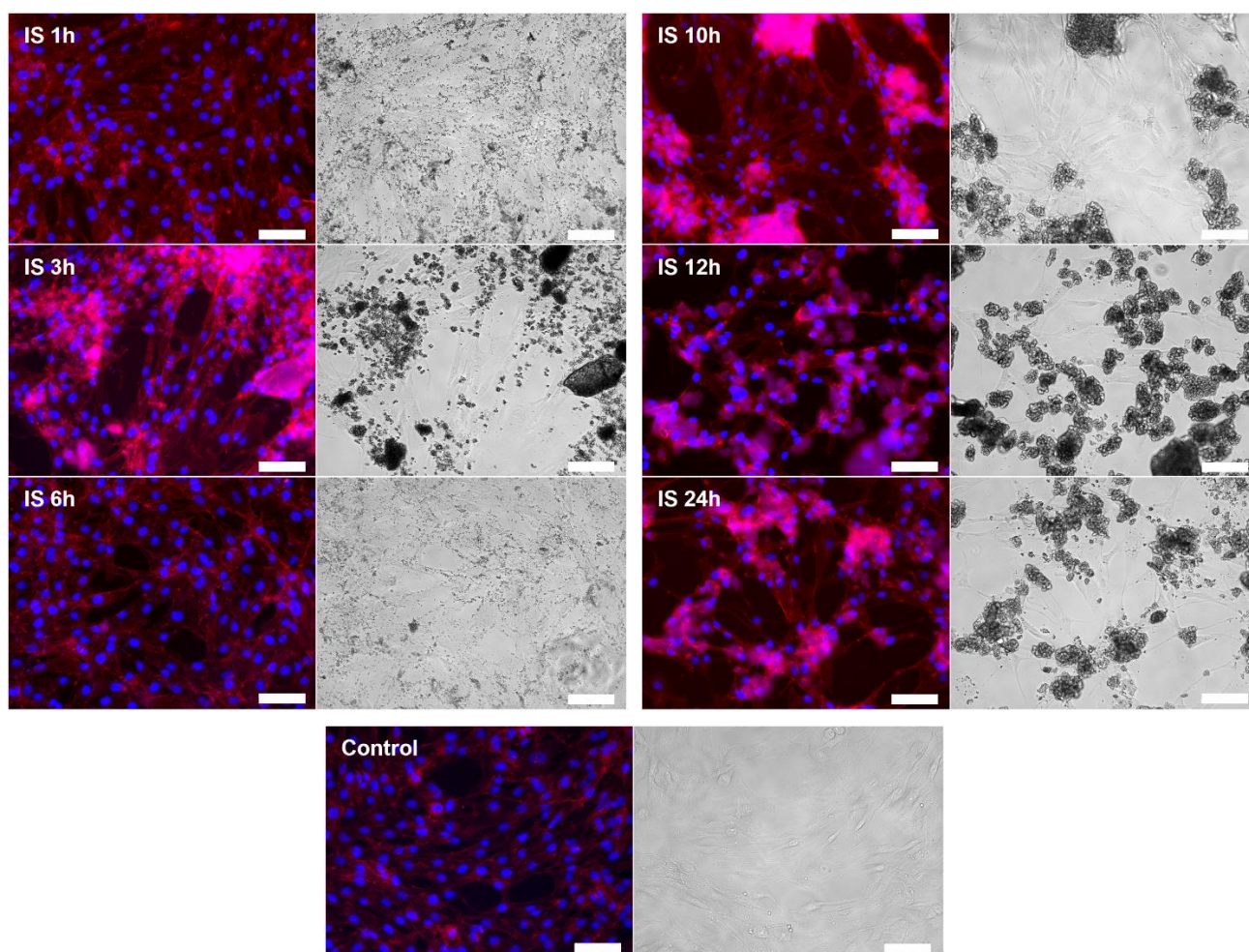


Figure S24. hBMSCs morphology on the third day of cultivation in direct contact with initial synthesis OCP samples in the concentration of 0.5 mg/mL. *Control* represents cells on polystyrene. Immunofluorescent (DAPI – blue, phalloidin – red) and bright-field microscopy. Image bar scale: 125 μ m.